Food Chemistry: X 15 (2022) 100396

Contents lists available at ScienceDirect

Food Chemistry: X

journal homepage: www.sciencedirect.com/journal/food-chemistry-x

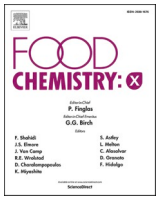

Hydrophobic bonds-dominated key off-odors/silver carp myofibrillar protein interactions, and their binding characteristics at cold storage and oral temperatures

Chao Xue [a,b,1], Juan You [a,b,1], Huimin Zhang [a,b], Liyuan Zhao [a,b], Shanbai Xiong [a,b], Tao Yin [a,b], Qilin Huang [a,b,*]

[a] College of Food Science and Technology, and MOE Key Laboratory of Environment Correlative Dietology, Huazhong Agricultural University, Wuhan 430070, China
[b] National R&D Branch Center for Conventional Freshwater Fish Processing, Wuhan 430070, China

ARTICLE INFO

Keywords:
Myofibrillar protein
Off-odors
Interaction mechanism
Fluorescence spectroscopic analysis
Molecular dynamics simulation

Chemical compounds used in the study:
Sodium chloride (PubChem CID: 5234)
Hexanal (PubChem CID: 6184)
1-octen-3-ol (PubChem CID: 18827)
Nonanal (PubChem CID: 31289)
Methanol (PubChem CID: 887)
Hydrochloric acid (PubChem CID: 313)
Tris (Hydroxymethyl) aminomethane (PubChem CID: 6503)
Monosodium phosphate (PubChem CID: 23672064).

ABSTRACT

This study revealed the interaction mechanism between silver carp myofibrillar protein (MP) and key off-odors by combining fluorescence spectroscopy with molecular dynamics (MD) simulation. Spectroscopic results exhibited a dynamic quenching mechanism between MP and off-odors. Thermodynamic analysis indicated that the MP/off-odors interaction was spontaneous ($\Delta G^\circ < 0$) and dominated by hydrophobic interactions ($\Delta H^\circ > 0$, $\Delta S^\circ > 0$). Meanwhile, the binding affinity was in the order of nonanal (n = 1.38) > hexanal (n = 0.89) > 1-octen-3-ol (n = 0.65), which was further verified by the MD results. Among off-odors, nonanal had the highest binding energy with myosin (8105.66 kJ/mol) and formed more hydrophobic binding sites to Trp residues in myosin head (e.g., Trp820 and Trp822), thereby changing myosin conformations via both physical and chemical interactions. Additionally, higher binding energies of myosin/off-odors were observed at oral temperature (37 °C) than at cold storage temperature (4 °C), implying that less off-odors were released at 37 °C.

Introduction

Silver carp (*Hypophthalmichthys molitrix*) is recognized as a good source of high-quality protein because of its great production and moderate price (An, Qian, Alcazar Magana, Xiong, & Qian, 2020; Zhang et al., 2019). However, due to the living environment and physiological-biochemical characteristics, silver carp usually has a large number of unacceptable flavors on the surface and inside. In order to understand these off-odors, researchers have explored their composition, and the main components of the mixed fishy flavor have been reported to include the volatile compounds, such as aldehydes, ketones, and alcohols. Fu, Xu, and Wang (2009) found that nonanal, 1-octen-3-ol, and hexanal contributed to the earthy odor and oily of silver carp mince. Similar results were also observed in our previous study (Zhang, Wu et al., 2020), which showed that these three compounds had a significant influence in the formation of silver carp's integral off-odor characteristics. Gu et al. (2020) also defined 1-octen-3-ol and nonanal as main fishy off-odors of silver carp for the study of binding capacity of surimi protein to flavor compounds.

As an essential component of the food, the interaction between food protein and flavors has become a growing focus of research (Cao, Zhou, Wang, Sun, & Pan, 2018; Fischer, Cachon, & Cayot, 2021; Lv et al., 2017). Myofibrillar protein (MP) accounts for ~ 55–65 % of total fish proteins and is vital to the flavor release and gel properties of fish products. It can interplay with flavor compounds via reversible (hydrogen bond, hydrophobic interaction, electrostatic interaction, etc.)

* Corresponding author at: College of Food Science and Technology, and MOE Key Laboratory of Environment Correlative Dietology; National R&D Branch Center for Conventional Freshwater Fish Processing, Huazhong Agricultural University, Wuhan 430070, China.
E-mail address: hql@mail.hzau.edu.cn (Q. Huang).
[1] Co-first author contributed equally to this work.

https://doi.org/10.1016/j.fochx.2022.100396
Received 25 May 2022; Received in revised form 12 July 2022; Accepted 14 July 2022
Available online 16 July 2022

or irreversible (covalent bond) binding forces. For instance, grass carp MP was capable of interplaying with aldehydes via hydrophobic interaction and covalent binding, and hydrogen bond was reported to be responsible for the adsorption of myofibrillar protein to alcohols (Xu et al., 2020; Yang et al., 2017). Meanwhile, the binding capacity between MP and volatile compounds has been reported to be influenced by a variety of environmental factors, such as MP concentration, temperature, exogenous additives, microwave, and ultrasound, etc. (Han, Cai, Cheng, & Sun, 2019; Pérez-Juan, Flores, & Toldrá, 2007; Xu et al., 2021; Xue et al., 2021). These factors could induce changes in the protein tertiary structure and flavor profiles of fish products during food processing. However, to our knowledge, little information is still available regarding the binding characteristics underlying the interactions between fish MP and flavor compounds (especially off-odors) during food processing. Probing this knowledge can aid in the better understanding of the interaction between MP and off-odors, and provide a further alternative for an effective deodorization of fish products.

The propose of the present work was to establish clear and accurate linkages between the key off-odors (hexanal, nonanal, 1-octen-3-ol) and silver carp myofibrillar protein (MP) at cold storage and oral temperatures (277 and 310 K). Consumers may perceive off-odors at these two temperatures when buying or eating fish products. To this end, fluorescence spectroscopic analysis was applied to detect the interaction relationship between off-odors and protein fluorophores. Meanwhile, due to the difficulty to observe the atomic level interactions through experiments alone, molecular dynamics (MD) simulation was adopted to investigate the binding properties and position between off-odors and protein at two temperatures. This work not only reveals the binding mechanism between fish proteins and off-odors at cold storage and oral temperatures, but also provides an alternative for an effective deodorization to improve the flavor profile of freshwater fish products.

Materials and methods

Materials

Fresh silver carp were obtained from a local aquatic products market (Wuhan, Hubei, China), and transported to the lab alive in an aquarium by truck within 20 min. Oxygen was supplied continuously during transportation and pre-slaughter. The silver carp were instantly stunned by a blow to the head, followed by beheading, scaling, eviscerating, filleting and washing. These procedures were carried out in accordance with research protocols approved by the Institutional Animal Care and Use Committee of Huazhong Agricultural University (Wuhan, China). Standard compounds used in this study were chromatographic grade: hexanal (≥99 %) provided by Aladdin Co., ltd (Shanghai, China); 1-octen-3-ol (>98 %) and nonanal (>95 %) from Shanghai Yuanye Biotechnology Co., ltd (Shanghai, China); and methanol (≥99.8 %) supplied by Sinopharm Chemical Reagent Co., ltd (Shanghai, China). Other required chemicals were of analytical grade and provided by Sinopharm Chemical Reagent Co., ltd.

MP extraction

MP was extracted from silver carp using our previously method (Xue et al., 2021).

Solution preparation of off-odor compounds and MP

After dissolving three off-odors in methanol completely, hexanal, 1-octen-3-ol and nonanal were diluted in deionized water to 0.10, 0.08 and 0.04 mmol/mL respectively.

MP solution was diluted to 0.5 mg/mL with the high-salt phosphate buffer (0.6 mol/L NaCl, 15.5 mmol/L $Na_2HPO_4{\cdot}12H_2O$, 3.38 mmol/L $NaH_2PO_4{\cdot}2H_2O$, pH 7.5), followed by transferring MP solution (1 mL) to 10 mL colorimetric tubes and mixing the solution with a different amount of off-odor compounds stock solutions. Next, the mixture was diluted to 5 mL to obtain the final three off-odors at concentrations of 0, 0.07, 0.14, 0.28, 0.42, 0.56, 0.70, 1.40, 2.10, 2.80, 3.50 and 4.20 mmol/L with the constant MP content of 0.1 mg/mL, which was selected based on the results of our pre-experiments. Finally, the mixed solution was well shaken and kept static at 277 and 310 K for 60 min for the following measurements.

Fluorescence spectra analysis of the interaction between MP and off-odors

Fluorescence quenching was obtained on a fluorescence spectrophotometer (F-4600, Hitachi, Japan). The fluorescence quenching spectra at 277 and 310 K were evaluated with the excitation wavelengths at 280 nm and emission wavelengths ranging from 290 ~ 450 nm. The slit widths were 5.0 nm.

Stern-Volmer equation (Eq. (1)) was selected to evaluate the quenching mechanism between three off-odor compounds and MP (Dai et al., 2017).

$$F_0/F = 1 + K_q\tau_0[Q] = 1 + K_{sv}[Q] \quad (1)$$

In Eq. (1), F_0 and F denote the fluorescence intensity without or with off-odors, respectively; K_q represents the quenching rate constant; K_{SV} represents the Stern-Volmer constant; [Q], the quencher concentration. τ_0, the average fluorescence molecule lifetime in the absence of off-odors;

Meanwhile, binding properties of the MP/off-odors complex was further estimated applying double logarithm regression curve using Equation (2):

$$\log(F_0 - F)/F = \log K + n\log[Q] \quad (2)$$

In this equation, K is the binding constant; n represents the number of binding sites of MP/off-odors complex.

To further investigate the interaction forces existed between off-odors and MP, thermodynamic parameters were calculated by Equations (3) and (4).

$$lnK = \frac{\Delta S^\circ}{R} - \frac{\Delta H^\circ}{RT} \quad (3)$$

$$\Delta G^\circ = \Delta H^\circ - T\Delta S^\circ \quad (4)$$

where ΔS°, ΔH°, ΔG° represent entropy change, enthalpy change, and Gibbs free energy change, respectively. K is the association constant at the given temperature; R represents the gas constant (8.314 J mol^{-1} K^{-1}); (Bijari et al., 2013).

Synchronous fluorescence spectra analysis of the interaction between MP and off-odors

The synchronous fluorescence spectra of the protein/off-odors were obtained in the fluorescence spectrophotometer (F-4600, Hitachi, Japan) with the settings of $\Delta\lambda$ = 15 and 60 nm. The the emission wavelength ranged from 220 ~ 450 nm, and the slit widths were 5.0 nm.

Computational studies of molecular dynamics

The sequence of MP in silver carp has not been reported to date, and no relevant template of MP was found in the Protein Data Bank (PDB) or other databases. Therefore, to further evaluate the main binding force and interaction properties between MP and off-odors, MD simulations of myosin (as the typical representative) at 277 and 310 K were conducted by the computational studies.

Homology modeling and model validation of protein structure

The myosin heavy chain's amino acid sequence was obtained from the National Center for Biotechnology Information (NCBI, GenBank:

BAF93224.1), and used for homology modeling of myosin head and MD simulation. Normally, identifying the best template structure is the first and most important step in homology modeling. In this study, the basic local alignment search tool (BLAST) method was used to screen suitable template proteins from the PDB database, and the results showed that 5TBY (Human β-cardiac myosin interacting-heads motif structure, https://www.rcsb.org/structure/5TBY) had 75.05 % sequence identity with our myosin sequence, indicating that 5TBY was an ideal template for the modeling of myosin head. Meanwhile, the three-dimensional model structure of myosin head (1 ~ 958 amino acids) was built and optimized by using Yet Another Scientific Artificial Reality Application software (YASARA, http://www.yasara.org/). Myosin tails (959 ~ 1932 amino acids) were constructed by CCBuilder 2.0 (coiledcoils.chm.bris.ac.uk/ccbuilder2/builder). MD simulation of the myosin head and tails were performed separately. Supplementary Fig. 1 shows the whole 3D myosin model in the YASARA software, with a head region (Myosin1) and a rodlike tail portion as a "coiled coil" of α-helix.

The program ERRAT is usually used to assess the distribution of different types of atoms in protein models (Al-Moubarak & Simons, 2011). In this study, the reliability of the myosin model was evaluated using ERRAT program, and the results showed that the overall quality of the myosin factor was good with a score of 88.6, indicating the high accuracy of the myosin model (Supplementary Fig. 2).

MD simulation

The interactions of the myosin model with three off-odors were investigated by YASARA software at the temperatures of 277 and 310 K and the pressure of 1 atm https://www.yasara.org. Specifically, the myosin model was assigned for Amber14 force field (Zhang et al., 2017), and the field parameters were developed by the AutoSMILES algorithm. The myosin model and off-odor compounds were solvated by cubic boxes of TIP3P water (rigid water model with 3 points of intermolecular transferable sites) with Na^+ and Cl^+. Then, the whole system was subjected to energy minimization to eliminate energetically unfavorable interactions between ions and water molecules. The simulation systems for myosin-hexanal, myosin-(1-octen-3-ol) and myosin-nonanal simulation systems contained 852669, 818841 and 810758 atoms, respectively. The simulation of myosin/off-odors was stabilized for 10 ns to restrain the coordinates of the backbone chain atoms of off-odors and protein and ensure the sufficient release of side chain atoms, followed by a 50 ns unrestrained MD simulation for production. A time step of 1.25 and 2.5 fs was used for binding and non-binding interactions, respectively.

The sum of the contributions of all hydrophobic atom pairs with distance determined the total hydrophobic bond strength, and the contribution of each hydrophobic atom pair in a value range 0 ~ 1. Generally, interaction strengths > 5.0 imply strongly interacting residues.

The binding energy (E_{bind}) was calculated by the YASARA software using the following equation (Eq. 5):

$$E_{bind} = E_{pot_{complex}} + E_{sol_{complex}} - E_{pot_{myosin}} - E_{sol_{myosin}} - E_{pot_{off-odors}} - E_{sol_{off-odors}}$$

where $E_{pot\text{-}complex}$, $E_{pot\text{-}myosin}$ and $E_{pot\text{-}(off\text{-}odors)}$ are the potential energy of the complex and myosin and off-odors; $E_{sol\text{-}complex}$, $E_{sol\text{-}myosin}$ and $E_{sol\text{-}(off\text{-}odors)}$ are the solvent energy of the complex and myosin and off-odors.

Finally, the lowest binding energy and maximum docking number were used to find the optimum binding poses of Myosin1 and off-odors.

Statistical analysis

All texts were performed in triplicate and repeated in three independent batches of samples. Statistically significant differences were determined at a significance level of 0.05 using Duncan's multiple range tests by SPSS 22.0 (SPSS Inc., Illinois, USA). Origin 9.0 (Origin Lab Inc., Massachusetts, USA) was used to plot and analyze the data.

Results and discussion

Fluorescence quenching mechanism

Fluorescence spectroscopy is a very useful methods to evaluate the conformational changes of macromolecule complexes. The intrinsic fluorescence in protein include: tryptophan (Trp), phenylalanine (Phe) and tyrosine (Tyr) residues, with Trp residues as the primary contributor to fluorescence quenching. The alterations in protein often result in changes in the emission spectra of tryptophan. The fluorescence spectra of MP as the function of concentrations of hexanal, nonanal (0.00–2.10 mmol/L) and 1-octen-3-ol (0.00–4.20 mmol/L) are shown in Fig. 1a-c. When excited at 280 nm, a strong fluorescence emission of MP was observed at 330 nm. Meanwhile, MP showed gradual attenuation in the fluorescence intensity with the concentration increase in off-odors, indicating that all three off-odor compounds could quench the intrinsic fluorescence of MP and change its micro-environment (Jayabharathi, Thanikachalam, Perumal, & Srinivasan, 2011). Furthermore, with the increase in the off-odor concentrations, the fluorescence intensity was more significantly inhibited in the MP-nonanal complex (Fig. 1c) than in the MP-hexanal or MP-(1-octen-3-ol) complex (Fig. 1a and b), inferring that nonanal had a more significant quenching effect than hexanal or 1-octen-3-ol on the intrinsic fluorescence of MP, with a stronger bond with MP. Meanwhile, a higher concentration of 1-octen-3-ol was required to achieve the same degree of quenching as hexanal, verifying the weakest binding capacity of 1-octen-3-ol to MP within three off-odors.

Fluorescence quenching is defined as a decreasing process of the fluorescence intensity of a sample. Generally, fluorescence quenching mainly includes dynamic and static quenching or their co-existence (Wu et al., 2019). As shown in Fig. 1 (inserts), the correlation coefficients ranged from 0.9711 to 0.9981, indicating the linearity in the plot of F_0/F against [Q] was credible, and Stern-Volmer was sufficient to describe the quenching mechanism of MP/off-odors complex. Meanwhile, the curves presented good linearity (Fig. 1 insets), indicating a single type of quenching mechanism between MP and the three off-odors (Shu et al., 2015).

Static quenching refers to the formation of nonfluorescent complexes between quenchers and fluorescence macromolecules in the ground state, which does not rely on diffusion or molecular collision, while dynamic quenching refers to the interaction between a quencher and a fluorophore in the excited state, and can be prompted by higher temperature to increase the quenching constant (Shu et al., 2015). The quenching rate constants (K_q) and quenching constants (K_{SV}) at 277 and 310 K are also listed in Table 1. It was shown that, in the presence of off-odor compounds, the K_{SV} values all increased with the temperature elevated from 277 to 310 K, indicating that dynamic quenching occurred in the binding between these three off-odor compounds and MP. Interestingly, the K_q values of nonanal at 277 and 310 K (9.57×10^{10}, 2.19×10^{11} L/mol·s) were higher than the maximum scatter collision quenching constant (2.0×10^{10} L/mol·s) for biomolecules with different quenchers, so it could be inferred as static quenching (Shu et al., 2015). This contradiction might be due to the complexity of MP. The constituents of MP (myosin and actin) were likely to show a variety of spectral properties when interacting with ligand molecules (Meng et al., 2021). Wu et al. (2019) deemed that, in this case, the K_q values of other quenchers with similar biopolymers should also be used as a reference for determining the quenching mechanism. In the present study, nonanal had lower K_q values at 277 and 310 K than the other compounds considered as static quenching mechanism for fish myofibrillar protein, such as chlorogenic acid (5.562×10^{14}), quercetin (5.176×10^{14}) (Xie et al., 2020), and curcumin ($1.58 \pm 0.11 \times 10^{12}$) (Wu et al., 2021). Therefore, the interaction mechanism of nonanal and MP could also be determined as dynamic quenching mechanism.

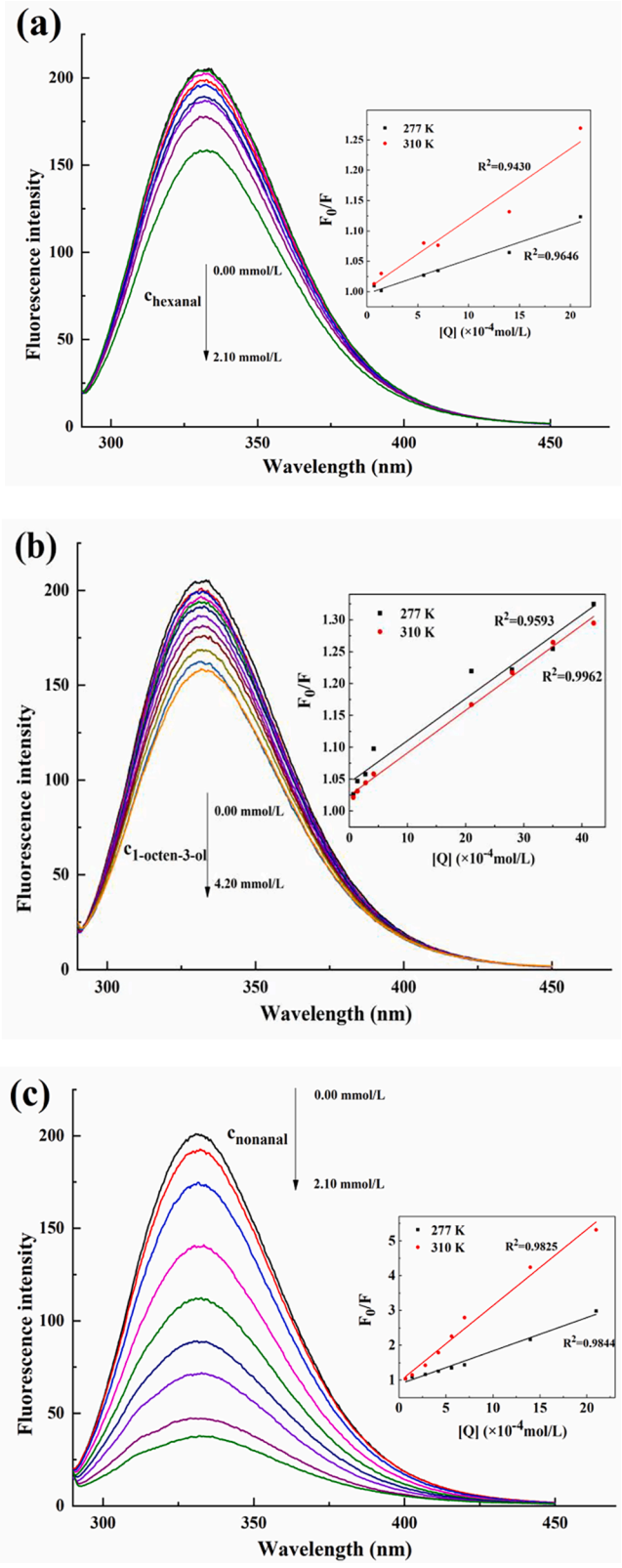

Fig. 1. Fluorescence emission spectra of the MP in the presence of increasing amounts of quenchers. (a) hexanal, (b) 1-octen-3-ol, (c) nonanal.

Interaction parameters for MP/off-odors complex

Generally, weak binding tends to cause the release of off-odor compounds, while tight binding can inhibit the release and decrease the perception of off-odors. Table 1 shows the K and n values of MP/off-odors interactions at 277 and 310 K obtained from the intercept and slope, and the correlation coefficients ranged from 0.9781 ~ 0.9964, indicating that the binding of MP/off-odors agreed well with the model outlined in Eq. (2). At 277 K, MP-nonanal showed the highest binding constant, reaching 2083 L/mol, implying strong binding interactions between MP and nonanal (Table 1). Moreover, it is worth noting that the binding constant of off-odors increased with the rise in temperature, indicating an increment in the stability of the MP/off-odors complex. Specifically, hexanal and nonanal showed higher K values than 1-octen-3-ol at 277 and 310 K, illustrating a stronger binding affinity of MP for aldehydes than MP-(1-octen-3-ol), which was more pronounced at the higher temperature (310 K). Furthermore, the highest binding constant was observed in the MP-nonanal complex, probably due to the irreversible covalent bonds formed between aldehydes and proteins. Meanwhile, nonanal has a longer carbon chain than hexanal, making the former easier to interact with proteins via hydrophobic interactions (Weel et al., 2003).

Heating could induce the MP to denature, aggregate, and form a cross-linked and continuous gel network. This explained why the number of protein/off-odors binding sites (n) was increased with the temperature rose from 277 to 310 K (Table 1). Huang, Zeng, Xiong, and Huang (2016) reported that internal hydrogen bonds of MP were destabilized with the temperature rose from 5 to 40 °C, resulting in the unfolding of MP macromolecules. Such unfolding consequently led to the exposure of hydrophobic side chains in some amino acid residues, thereby improving the binding affinity of MP and off-odors. This suggest that, off-odors may release less at oral temperature than at cold storage temperature.

Moreover, the n values at 277 and 310 K were close to or $>$ 1 for hexanal and nonanal, respectively, suggesting the binding of hexanal and nonanal to MP might be 1:1. However, both the K and n values of the MP-(1-octen-3-ol) complex were obviously lower than MP-nonanal or MP-hexanal, indicating the inferior binding ability of 1-octen-3-ol to MP. This showed a good agreement with the results of fluorescence quenching mechanism.

Thermodynamic parameters of MP/off-odors complex

Interaction thermodynamics was further studied to obtain an insight into the binding behaviors and reveal the mechanisms involved in the binding process. Table 1 also lists the thermodynamic parameters (ΔG°, ΔH° and ΔS°) of MP/off-odors complex at 277 and 310 K. The ΔG° is a critical factor for determining the spontaneity degree of the adsorption process. At 277 and 310 K, all ΔG° values were found to be negative, suggesting that the MP/off-odors interactions were all thermodynamically feasible and spontaneous (Yousef, El-Eswed, & Ala'a, 2011). Moreover, all the three off-odor compounds showed lower ΔG° values at 310 K than at 277 K, indicating that the binding of off-odor compounds to MP was more favorable at high temperature and belonged to endothermic process. Additionally, the ΔH° values were 36.77, 4.42 and 58.30 kJ/mol for of hexanal, 1-octen-3-ol and nonanal, respectively, and the positive ΔH° value also indicated the endothermic nature for the interaction of the three off-odors with MP (Liu, Ying, Sanguansri, & Augustin, 2019). Meanwhile, these parameters can also be used to reveal the nature of binding force. Generally, the magnitude of ΔH° is $<$ 40 kJ/mol for physical interaction. Such process is hold by comparative weaker forces (i.e., Van der Waal force), while chemical interaction involves the formation of covalent bonds. In the present study, both the ΔH° value of hexanal and 1-octen-3-ol were lower than 40 kJ/mol (Table 1), suggesting that physical interaction played a dominate role in the MP-hexanal and MP-(1-octen-3-ol) interactions (Tran, You, & Chao, 2016). This physical interaction is susceptible to protein structural changes induced by the environments, thereby impacting the flavor binding or release. Furthermore, nonanal had a ΔH° value higher than 40 kJ/mol, demonstrating the existence of both physical and chemical

Table 1
Stern-Volmer quenching constants, binding constant (K), binding site number (n) and thermodynamic parameters of MP-hexanal, MP-(1-octen-3-ol) and MP-nonanal systems at different temperatures.

System	T (K)	K_{SV} (L/mol)	K_q (L/mol·s)	r_1	K (L/mol)	n	ΔG° (kJ/mol)	ΔH° (kJ/mol)	ΔS° (J/mol·k)	r_2
MP-hexanal	277	56.4	5.64×10^9	0.9822	11.70	0.80	−5.67	36.77	153.14	0.9874
	310	116.0	1.16×10^{10}	0.9711	63.94	0.89	−10.72			0.9880
MP-(1-octen-3-ol)	277	65.9	6.59×10^9	0.9794	8.06	0.58	−4.81	4.42	33.32	0.9781
	310	66.9	6.69×10^9	0.9981	9.89	0.65	−5.91			0.9964
MP-nonanal	277	956.6	9.57×10^{10}	0.9921	2083.05	1.15	−17.61	58.30	273.87	0.9874
	310	2.19×10^3	2.19×10^{11}	0.9912	30768.05	1.38	−26.65			0.9887

interaction between the nonanal and MP. It was probably due to the existence of non-covalent interactions and strong Schiff base reaction between the lysine residues of the protein and aldehyde functional groups of nonanal. Such reaction may also cause changes in the flavor profile of fish products, due to the consumption of nonanal and the formation of new substances.

The major force between the off-odors and MP can be determined by analyzing thermodynamic characteristics. For ligand–protein interaction, the main force can be evaluated as follows: 1) $\Delta H^\circ < 0$ and $\Delta S^\circ < 0$ exhibit the involvement of both Van der Waals force and hydrogen bonding in the interaction; 2) $\Delta H^\circ > 0$ and $\Delta S^\circ > 0$ represent hydrophobic interaction; 3) $\Delta H^\circ < 0$ and $\Delta S^\circ > 0$ signify electrostatic interaction (Li, Zhu, Jin, & Yao, 2007). In Table 1, the positive ΔH° (36.77, 4.42 and 58.30 kJ/mol) and ΔS° (153.14, 33.32 and 273.87 J/mol·k) values of the three complexes clearly demonstrated that hydrophobic interactions played a key role in the MP/off-odors binding process. Moreover, hydrogen bond interaction may also exist between 1-octen-3-ol and MP due to the presence of hydroxyl. Yang et al. (2017) suggested that the changes in hydrogen bonding could significantly decrease the binding ability of duck protein to 1-octen-3-ol and 1-octanol.

Synchronous fluorescence spectroscopy

Synchronous fluorescence is a very powerful tool for studying the conformation of chromophore molecules in the micro-environment (Klajnert & Bryszewska, 2002). Fig. 2 exhibits the spectra for the interaction of MP with various concentrations of off-odor compounds. In Fig. 2a, c, e, the fluorescence intensity of Tyr residues was seen to be weaker than that of Trp residues (Fig. 2b, d, f), suggesting that Trp residues were the dominant contributor to the fluorescence intensity.

In Fig. 2a, b, it was shown that, with the rise in hexanal concentration, the fluorescence intensity declined in both Trp and Tyr residues, with a more significant decrease in the former, indicating that the fluorescence intensity of these two amino acid residues were both weakened due to the interaction between hexanal and MP. Similar results were also observed in Fig. 2c-f, illustrating that 1-octen-3-ol (Fig. 2c, d) and nonanal (Fig. 2e, f) could bind to MP and weaken the fluorescence intensity of Trp and Tyr residues, but no significant decrease was observed in the Tyr fluorescence intensity (Fig. 2c), in accordance with the results of previous spectroscopic study on the binding of polyphenols to grass carp myofibrillar protein (Xie et al., 2020) and theaflavin-3,3′-digallate to bovine serum albumin (BSA) (Yu et al., 2022). Collectively, nonanal showed the greatest decrease in the fluorescence intensity of both residues, followed by hexanal and 1-octen-3-ol, consistent with previous fluorescence quenching results.

In synchronous fluorescence spectra, the change in the polarity around the conformation of the fluorophore can be inferred from the change in the maximum fluorescence emission wavelength ($\lambda_{em\ max}$), and the shift of its position denotes the changes of polarity around these fluorophore molecules. Generally, the blue shift of $\lambda_{em\ max}$ suggests the increase in the hydrophobic micro-environment around Tyr or Trp residues, whereas the red shift suggests that a part of Trp or Tyr residues have been exposed to the hydrophilic phase. In Fig. 2, the $\lambda_{em\ max}$ of Tyr residues showed no obvious change after adding different concentrations of hexanal (Fig. 2a), 1-octen-3-ol (Fig. 2c) and nonanal (Fig. 2e), indicating that the micro-environment surrounding Tyr residue was not changed markedly in the presence of these off-odor compounds. However, a slight blue-shift of $\lambda_{em\ max}$ in Trp was shown in nonanal (Fig. 2f), but not in hexanal (Fig. 2b) or 1-octen-3-ol (Fig. 2d), indicating the deformation of the MP conformation upon interaction with nonanal.

MD simulation of hydrophobic interactions between myosin and off-odors

MD simulation is a method commonly used to investigate the protein/small molecule interactions, allowing researchers to track the detailed binding properties and conformational changes over the required time span (Mohseni-Shahri, Moeinpour, & Nosrati, 2018). Scholars often use the main binding regions as representatives of complex structures to observe the important functional processes, such as ligand binding (J. Li et al., 2021; Wang et al., 2022). As an important constituent of MP, myosin has been found to play a vital role in releasing and binding of volatile compounds in meat products (He, Zhou, Li, & Zhou, 2021). Gu et al. (2020) found that myosin was the primary binding receptors for flavor compounds compared with other silver carp proteins (myofibrillar protein and actin). Therefore, silver carp myosin was considered as the representative of the MP and use to further understand the dominant interaction force (hydrophobic interaction) between protein and three off-odors. In Fig. 3, an upward trend was seen in the hydrophobic interaction signals between myosin and off-odors, consistent with the hydrophobic interaction trend in previous modeling study on the binding of curcumin to myosin heavy chain (Zhang, Sun et al., 2020). It is also found that the hydrophobic binding signals became almost stationary after 30 ns, indicating that our simulation time was sufficient. At the low simulation temperature (277 K), the hydrophobic binding strength of myosin for off-odors was in the order of nonanal > hexanal > 1-octen-3-ol, corresponding well with our fluorescence spectroscopic results. Meanwhile, higher hydrophobic interaction strengths between off-odors and myosin were also observed at a 310 K, which could be explained by the fact that heating (4 – 40 °C) could unfold the helical structure and increase the random coils of MP, leading to the exposure of hydrophobic side chains and an increase in hydrophobic binding sites (Xue et al., 2021). In this case, it may prevent the off-odors from being released at oral temperature by improving binding affinity.

MD simulation of binding energy in the interaction between myosin and off-odors

The energy provided by the interaction between different amino acids around the cavity of the target protein and screening molecule is known as binding energy. Fig. 4 shows the binding energy between off-odors and myosin determined by MD simulation. These residues provide energy through different interactions, such as hydrogen bonding, electrostatic interaction, hydrophobic interaction, etc. (Kumar et al., 2021). As shown in Fig. 4, the myosin-nonanal complex showed the highest binding energies at 277 and 310 K, followed by myosin-hexanal and myosin-(1-octen-3-ol) complexes. Meanwhile, increasing the simulation temperature could also increase the binding energy of myosin/off-odor complexes, showing a good agreement with the results obtained in the section 3.5, indicating that, compared with fish products at 277 K, off-

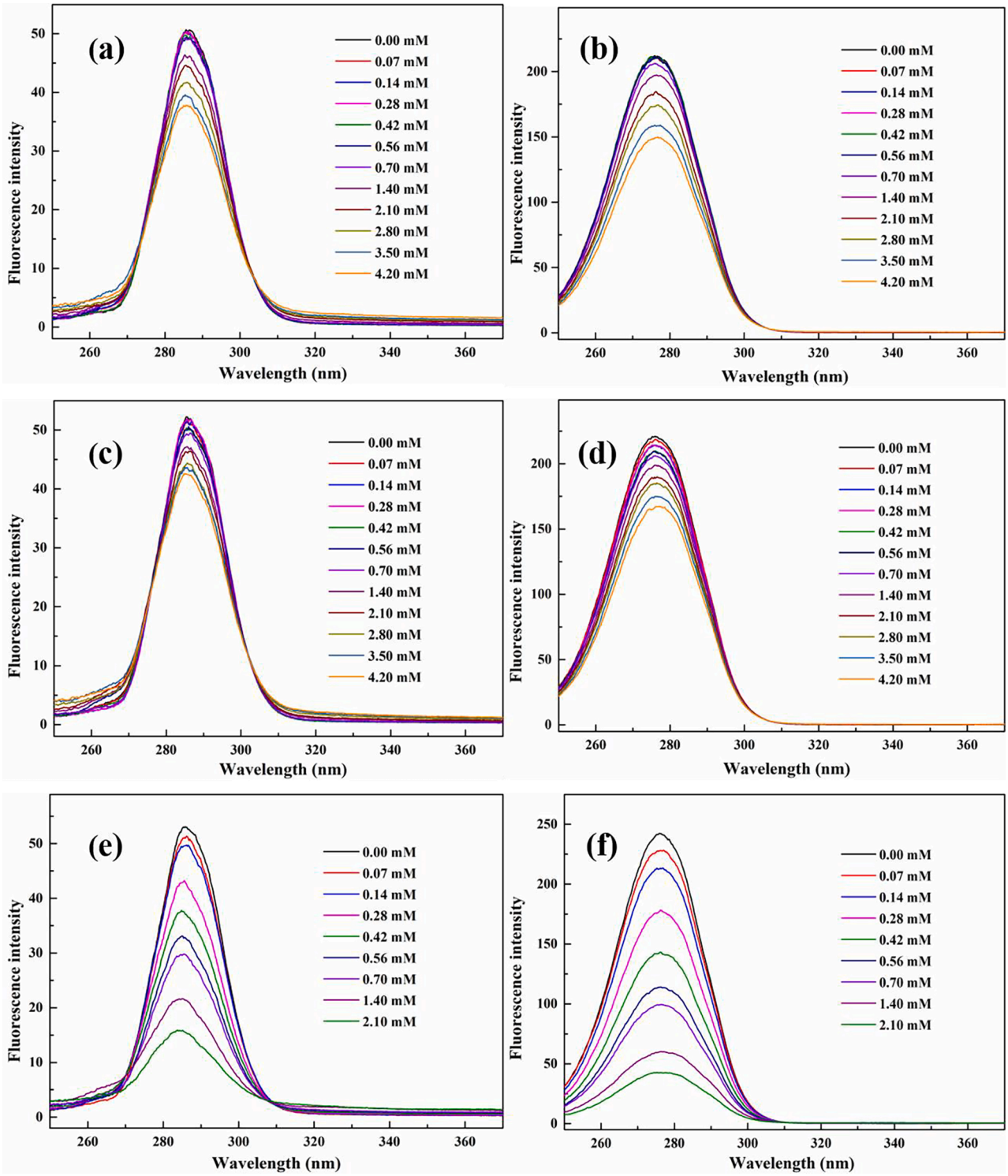

Fig. 2. Synchronous fluorescence spectra for MP interaction with various amounts of hexanal (a, b), 1-octen-3-ol (c, d) and nonanal (e, f); (a), (c), (e) $\Delta\lambda = 15$ nm, (b), (d), (f) $\Delta\lambda = 60$ nm.

odors might be easier to influence consumers' sensory perception of fish products in the oral cavity, due to a higher binding affinity. Moreover, note that the myosin-(1-octen-3-ol) complex had the minimal increase from 5134.38 to 5712.54 kJ/mol with the temperature elevated from 277 to 310 K. A possible explanation is that Schiff base reaction improve the binding strength of myosin-aldehydes, but 1-octen-3-ol could only bind to the protein through non-covalent interaction. The binding energy results also agreed well with the fluorescence spectroscopic results.

Binding poses analysis of the Myosin1/off-odors complex

Harrington and Rodgers (1984) reported that both the enzymatic active sites and the active binding regions of myosin are concentrated in the globular heads, so this section mainly focused on the interaction between Myosin1 and three off-odors. The interactions of the optimum binding conformation of off-odor compounds with the amino acid residues of myosin are shown in Fig. 5. Clearly, Myosin1 varied greatly in

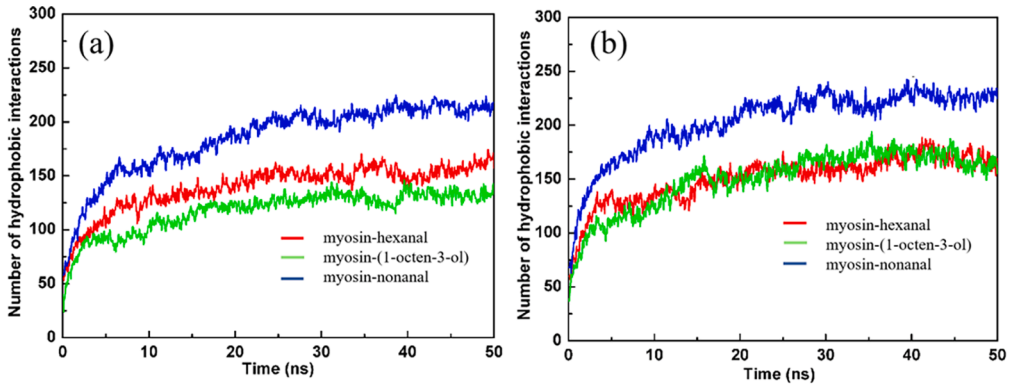

(c)

Temperatures	The average number of hydrophobic interactions of myosin-odors		
	myosin-hexanal	myosin-(1-octen-3-ol)	myosin-nonanal
277 K	150.56 ± 9.19 [b]	128.02 ± 7.16 [c]	202.62 ± 13.14 [a]
310 K	162.02 ± 10.52 [b]	164.67 ± 11.68 [c]	219.64 ± 11.57 [a]

Notes: Data are expressed as the mean ± standard deviation of three experiments.
Values in the same line followed by different letters were significantly different ($P < 0.05$).

Fig. 3. The hydrophobic binding strength of hydrophobic interactions between myosin and off-odors at different temperatures during simulation. (a) at 277 K, (b) at 310 K, and (c) the average number of hydrophobic interactions in the myosin-odors over the last 20 ns in simulation.

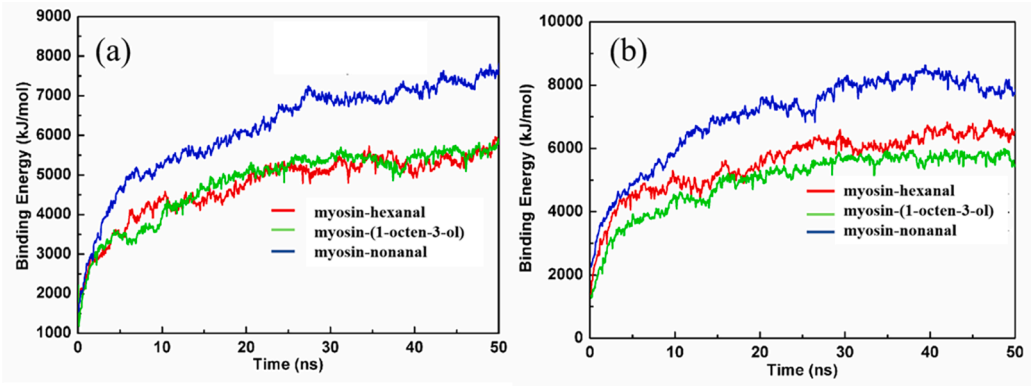

(c)

Temperatures	Binding energies of myosin-odors (kJ/mol)		
	myosin-hexanal	myosin-(1-octen-3-ol)	myosin-nonanal
277 K	5708.21 ± 163.97 [b]	5134.37 ± 208.64 [c]	7168.46 ± 533.96 [a]
310 K	6329.86 ± 262.94 [b]	5712.54 ± 149.04 [c]	8105.66 ± 228.01 [a]

Notes: Data are expressed as the mean ± standard deviation of three experiments.
Values in the same line followed by different letters were significantly different ($P < 0.05$).

Fig. 4. The binding energy of off-odors and myosin at different temperatures over the course of simulation. (a) at 277 K, (b) at 310 K, and (c) the total binding energy of off-odors and myosin.

the binding ability for the three off-odors. Specifically, after MD simulation, some hexanal and nonanal molecules were still dispersed in the box, while nearly all nonanal molecules were observed to bind on the surface of Myosin1 (some nonanal aggregated to form a spherical shape on the Myosin1 surface at 4 °C). Meanwhile, as shown in Fig. 5c-1, C-1, the binding of nonanal on the surface of Myosin1 was enhanced with the increase in temperature, resulting in the dissipation of the sphere and its even distribution on the surface of Myosin1, which was also observed in the binding of hexanal (Fig. 5a-1, A-1), but the binding of 1-octen-3-ol was not significantly improved.

High binding energy and strength made hydrophobic interactions the key contributor to protein-flavor stability. Therefore, myosin residues with the strongest hydrophobic binding capacity to off-odors were further investigated in this section. At 277 K, hexanal interacted with Leu613, Trp435, Met432, Met436, Phe338, Phe349, Thr350 and Ile346 (Fig. 5a-2, a-3); 1-octen-3-ol formed hydrophobic bonds with several amino acid residuals, including Trp108, Tyr10, Tyr105, Ile110, and Leu127 (Fig. 5b-2 b-3); nonanal formed strong hydrophobic bonds with the Myosin1 active site, with the residues including Val817, Trp820, Trp822, Lys824, Val825, Met823, and Lys830 (Fig. 5c-2, c-3). At 310 K,

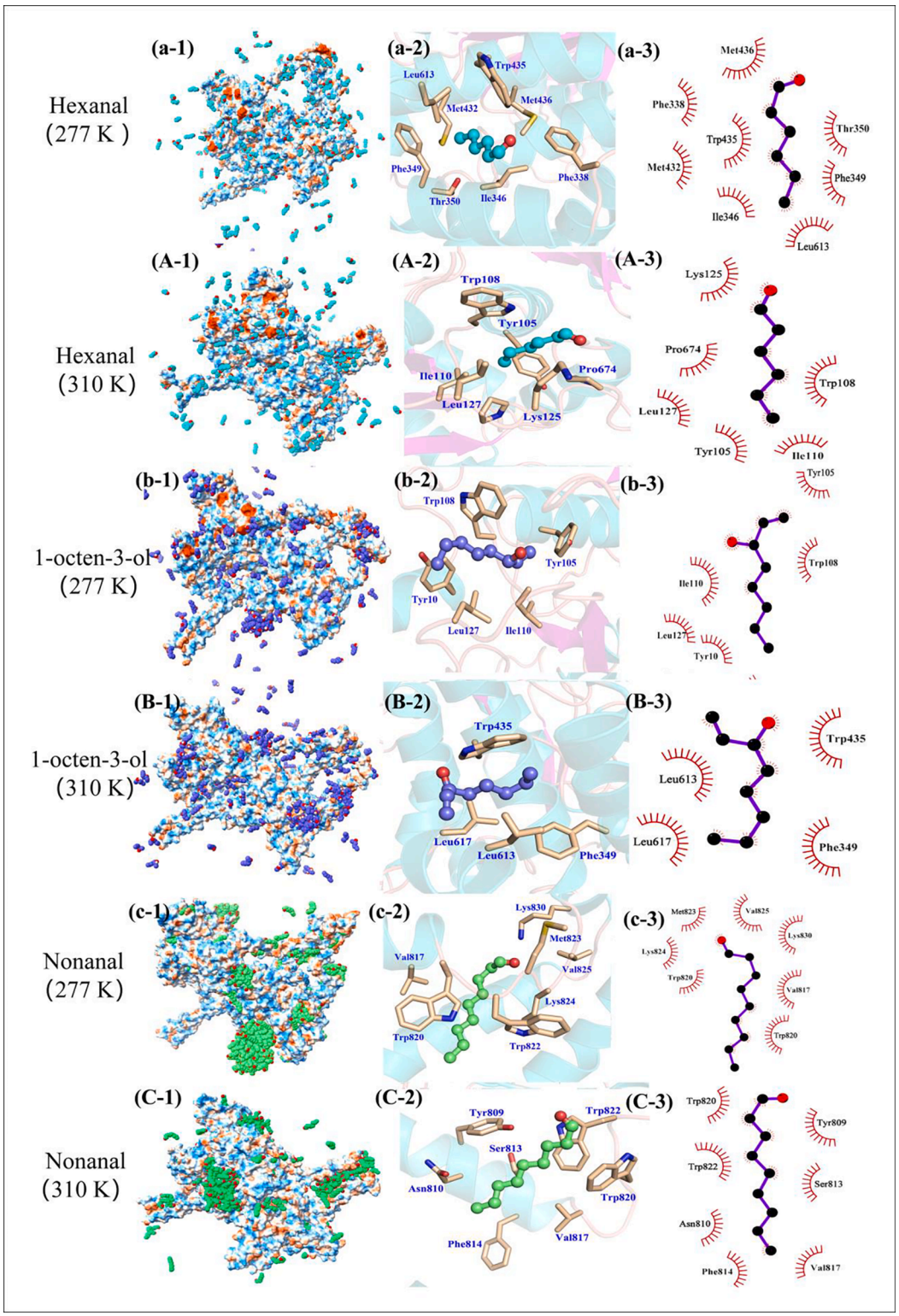

Fig. 5. The interactions of hexanal (blue, a1-a3 and A1-A3), 1-octen-3-ol (purple, b1-b3 and B1-B3) and nonanal (green, c1-c3 and C1-C3) with Myosin1 at different simulation temperatures (a, b, c at 277 K, and A, B, C at 310 K). a-1, b-1, c-1, A-1, B-1, C-1 represent the optimum binding conformations of off-odor compounds with Myosin1; a2-a3, b2-b3, c2-c3, A2-A3, B2-B3, *C*2-C3 represent the hydrophobic bonds of the optimum binding conformations of off-odor compounds with the amino acid residues of Myosin1. a-2, b-2, c-2, A-2, B-2, C-2: Three-dimensional binding conformation; a-3, b-3, c-3, A-3, B-3, C-3: Two-dimensional binding conformation. (For interpretation of the references to colour in this figure legend, the reader is referred to the web version of this article.)

hexanal had hydrophobic interactions with Trp108, Ile110, Tyr105, Lys125, Leu127 and Pro674 (Fig. 5A-2, A-3); 1-octen-3-ol bound to the residues Trp435, Leu613, Leu617, and Phe349 (Fig. 5B-2, B-3); and nonanal interacted with residues Tyr809, Trp822, Ser813, Trp820, Asn810, Val817 and Phe814 (Fig. 5C-2, C-3). The formation of these hydrophobic bonds reduced the influence of hydrophobic hydration and helped maintain the three-dimensional structure of the Myosin1/off-odors complex (Lv et al., 2022).

Furthermore, it is worth noting that off-odors could interact with Trp435, Trp108, Tyr10 and other residues of Myosin1, but these residues could be buried inside the newly formed Myosin1/off-odors complexes at a higher temperature and hardly be excited internally and emit fluorescence. Meanwhile, compared with 1-octen-3-ol and hexanal, nonanal interacted with more Trp residues in Myosin1 at the two temperatures (see Fig. 5), which explained why the nonanal addition resulted in stronger endogenous fluorescence quenching and blue shift of wavelength in the MP. Collectively, these results provided a solid structural foundation for explaining emission fluorescence quenching in the presence of off-odors.

Conclusions

Off-odors (hexanal, nonanal, and 1-octen-3-ol) could quench the intrinsic fluorescence of MP in a dynamic mode. Meanwhile, typical spontaneity and hydrophobic interactions were observed in the binding of MP and off-odors, with binding affinity in the order of nonanal > hexanal > 1-octen-3-ol. Moreover, off-odors had higher binding affinity with MP at 310 K, and MP-hexanal and MP-(1-octen-3-ol) interactions were mainly driven by physical interaction, in contrast to both chemical and physical interaction for the binding of nonanal to MP. Additionally, nonanal could induce changes in the conformation of MP and the polarity of the micro-environment around Trp residues by interacting with Trp residues via hydrophobic bonds. This study provided insights into the mechanism of protein/off-odors interactions and may contribute to the effective deodorization of fish products.

Ethical statement

This article does not contain any studies with human subjects. All fish handling procedures were conducted according to the research protocols approved by the Institutional Animal Care and Use Committee of Huazhong Agricultural University, Wuhan, China.

CRediT authorship contribution statement

Chao Xue: Methodology, Formal analysis, Investigation, Software. **Juan You:** Methodology, Writing – review & editing. **Huimin Zhang:** Methodology, Validation. **Liyuan Zhao:** Methodology, Formal analysis, Investigation. **Shanbai Xiong:** Methodology. **Tao Yin:** Validation. **Qilin Huang:** Project administration, Validation, Writing – review & editing, Funding acquisition.

Declaration of Competing Interest

The authors declare that they have no known competing financial interests or personal relationships that could have appeared to influence the work reported in this paper.

Acknowledgment

This research did not receive any specific grant from funding agencies in the public, commercial, or not-for-profit sectors.

Appendix A. Supplementary data

Supplementary data to this article can be found online at https://doi.org/10.1016/j.fochx.2022.100396.

References

Al-Moubarak, E., & Simons, C. (2011). A homology model for Clostridium difficile methionyl tRNA synthetase: Active site analysis and docking interactions. *Journal of Molecular Modeling, 17*(7), 1679–1693. https://doi.org/10.1007/s00894-010-0871-9

An, Y., Qian, Y. L., Alcazar Magana, A., Xiong, S., & Qian, M. C. (2020). Comparative characterization of aroma compounds in silver carp (*Hypophthalmichthys molitrix*), pacific whiting (*Merluccius productus*), and alaska pollock (*Theragra chalcogramma*) surimi by aroma extract dilution analysis, odor activity value, and aroma recombination studies. *Journal of Agricultural and Food Chemistry, 68*(38), 10403–10413. https://doi.org/10.1021/acs.jafc.9b07621

Bijari, N., Shokoohinia, Y., Ashrafi-Kooshk, M. R., Ranjbar, S., Parvaneh, S., Moieni-Arya, M., & Khodarahmi, R. (2013). Spectroscopic study of interaction between osthole and human serum albumin: Identification of possible binding site of the compound. *Journal of Luminescence, 143*, 328–336. https://doi.org/10.1016/j.jlumin.2013.04.045

Cao, J., Zhou, C., Wang, Y., Sun, Y., & Pan, D. (2018). The effect of oxidation on the structure of G-actin and its binding ability with aroma compounds in carp grass skeletal muscle. *Food Chemistry, 240*, 346–353. https://doi.org/10.1016/j.foodchem.2017.07.068

Dai, T., Yan, X., Li, Q., Li, T., Liu, C., McClements, D. J., & Chen, J. (2017). Characterization of binding interaction between rice glutelin and gallic acid: Multi-spectroscopic analyses and computational docking simulation. *Food Research International, 102*, 274–281. https://doi.org/10.1016/j.foodres.2017.09.020

Fischer, E., Cachon, R., & Cayot, N. (2021). Effects of extraction pH on the volatile compounds from pea protein isolate: Semi-Quantification method using HS-SPME-GC-MS. *Food Research International, 150*, Article 110760. https://doi.org/10.1016/j.foodres.2021.110760

Fu, X., Xu, S., & Wang, Z. (2009). Kinetics of lipid oxidation and off-odor formation in silver carp mince: The effect of lipoxygenase and hemoglobin. *Food Research International, 42*(1), 85–90. https://doi.org/10.1016/j.foodres.2008.09.004

Gu, S., Dai, W., Chong, Y., Lyu, F., Zhou, X., & Ding, Y. (2020). The binding of key fishy off-flavor compounds to silver carp proteins: A thermodynamic analysis. *RSC Advances, 10*(19), 11292–11299. https://doi.org/10.1039/D0RA01365J

Han, Z., Cai, M.j., Cheng, J. H., & Sun, D. W. (2019). Effects of microwave and water bath heating on the interactions between myofibrillar protein from beef and ketone flavour compounds. *International Journal of Food Science & Technology, 54*(5), 1787–1793. https://doi.org/10.1111/ijfs.14079

Harrington, W. F., & Rodgers, M. E. (1984). Myosin. *Annual Review of Biochemistry, 53*(1), 35–73.

He, Y., Zhou, C., Li, C., & Zhou, G. (2021). Effect of incubation temperature on the binding capacity of flavor compounds to myosin. *Food Chemistry, 346*, Article 128976. https://doi.org/10.1016/j.foodchem.2020.128976

Huang, J., Zeng, S., Xiong, S., & Huang, Q. (2016). Steady, dynamic, and creep-recovery rheological properties of myofibrillar protein from grass carp muscle. *Food Hydrocolloids, 61*, 48–56.

Jayabharathi, J., Thanikachalam, V., Perumal, M. V., & Srinivasan, N. (2011). Fluorescence resonance energy transfer from a bio-active imidazole derivative 2-(1-phenyl-1H-imidazo [4, 5-f][1, 10] phenanthrolin-2-yl) phenol to a bioactive indoloquinolizine system. *Spectrochimica Acta Part A: Molecular and Biomolecular Spectroscopy, 79*(1), 236–244. https://doi.org/10.1016/j.saa.2011.02.049

Klajnert, B., & Bryszewska, M. (2002). Fluorescence studies on PAMAM dendrimers interactions with bovine serum albumin. *Bioelectrochemistry, 55*(1–2), 33–35. https://doi.org/10.1016/S1567-5394(01)00170-0

Kumar, D., Kumari, K., Jayaraj, A., Kumar, V., Kumar, R. V., Dass, S. K., … Singh, P. (2021). Understanding the binding affinity of noscapines with protease of SARS-CoV-2 for COVID-19 using MD simulations at different temperatures. *Journal of Biomolecular Structure and Dynamics, 39*(7), 2659–2672. https://doi.org/10.1080/07391102.2020.1752310

Li, J., Munir, S., Yu, X., Yin, T., You, J., Liu, R., … Hu, Y. (2021). Double-crosslinked effect of TGase and EGCG on myofibrillar proteins gel based on physicochemical properties and molecular docking. *Food Chemistry, 345*, Article 128655. https://doi.org/10.1016/j.foodchem.2020.128655

Li, D., Zhu, J., Jin, J., & Yao, X. (2007). Studies on the binding of nevadensin to human serum albumin by molecular spectroscopy and modeling. *Journal of Molecular Structure, 846*(1–3), 34–41. https://doi.org/10.1016/j.molstruc.2007.01.020

Liu, Y., Ying, D., Sanguansri, L., & Augustin, M. A. (2019). Comparison of the adsorption behaviour of catechin onto cellulose and pectin. *Food Chemistry, 271*, 733–738. https://doi.org/10.1016/j.foodchem.2018.08.005

Lv, Y., Liang, Q., Li, Y., Liu, X., Zhang, D., & Li, X. (2022). Study of the binding mechanism between hydroxytyrosol and bovine serum albumin using multispectral and molecular docking. *Food Hydrocolloids, 122*, Article 107072. https://doi.org/10.1016/j.foodhyd.2021.107072

Lv, T., Wang, Y., Pan, D., Cao, J., Zhang, X., Sun, Y., … Liu, Y. (2017). Effect of trypsin treatments on the structure and binding capacity of volatile compounds of myosin. *Food Chemistry, 214*, 710–716. https://doi.org/10.1016/j.foodchem.2016.07.115

Meng, Y., Hao, L., Tan, Y., Yang, Y., Liu, L., Li, C., & Du, P. (2021). Noncovalent interaction of cyanidin-3-O-glucoside with whey protein isolate and β-lactoglobulin: Focus on fluorescence quenching and antioxidant properties. *LWT, 137*, Article 110386. https://doi.org/10.1016/j.lwt.2020.110386

Mohseni-Shahri, F. S., Moeinpour, F., & Nosrati, M. (2018). Spectroscopy and molecular dynamics simulation study on the interaction of sunset yellow food additive with pepsin. *International Journal of Biological Macromolecules, 115*, 273–280. https://doi.org/10.1016/j.ijbiomac.2018.04.080

Pérez-Juan, M., Flores, M., & Toldrá, F. (2007). Effect of ionic strength of different salts on the binding of volatile compounds to porcine soluble protein extracts in model systems. *Food Research International, 40*(6), 687–693. https://doi.org/10.1016/j.foodres.2006.11.013

Shu, Y., Xue, W., Xu, X., Jia, Z., Yao, X., Liu, S., & Liu, L. (2015). Interaction of erucic acid with bovine serum albumin using a multi-spectroscopic method and molecular docking technique. *Food Chemistry, 173*, 31–37. https://doi.org/10.1016/j.foodchem.2014.09.164

Tran, H. N., You, S.-J., & Chao, H.-P. (2016). Thermodynamic parameters of cadmium adsorption onto orange peel calculated from various methods: A comparison study. *Journal of Environmental Chemical Engineering, 4*(3), 2671–2682. https://doi.org/10.1016/j.jece.2016.05.009

Wang, H., Guan, H., Zhang, H., Liu, H., Chen, Q., & Kong, B. (2022). Elucidation of interaction mechanisms between myofibrillar proteins and ethyl octanoate by SPME-GC-MS, molecular docking and dynamics simulation. *LWT, 154*, Article 112787. https://doi.org/10.1016/j.lwt.2021.112787

Weel, K. G., Boelrijk, A. E., Burger, J. J., Claassen, N. E., Gruppen, H., Voragen, A. G., & Smit, G. (2003). Effect of whey protein on the in vivo release of aldehydes. *Journal of Agricultural and Food Chemistry, 51*(16), 4746–4752. https://doi.org/10.1021/jf034188s

Wu, C., Dong, H., Wang, P., Xu, X., Zhang, Y., & Li, Y. (2021). Insight into the effect of charge regulation on the binding mechanism of curcumin to myofibrillar protein. *Food Chemistry, 352*, Article 129395. https://doi.org/10.1016/j.foodchem.2021.129395

Wu, H., Zeng, W., Chen, G., Guo, Y., Yao, C., Li, J., & Liang, Z. (2019). Spectroscopic techniques investigation on the interaction of glucoamylase with 1-deoxynojirimycin: Mechanistic and conformational study. *Spectrochimica Acta Part A: Molecular and Biomolecular Spectroscopy, 206*, 613–621. https://doi.org/10.1016/j.saa.2018.08.013

Xie, W., Huang, Y., Xiang, Y., Xiong, S., Manyande, A., & Du, H. (2020). Insights into the binding mechanism of polyphenols and fish myofibrillar proteins explored using multi-spectroscopic methods. *Food and Bioprocess Technology, 13*(5), 797–806. https://doi.org/10.1007/s11947-020-02439-4

Xu, Y., Wang, R., Zhao, H., Zhao, J., Li, X., Yi, S., … Sun, X. (2020). Binding of aldehydes to myofibrillar proteins as affected by two-step heat treatments. *Journal of the Science of Food and Agriculture, 100*(3), 1195–1203. https://doi.org/10.1002/jsfa.10130

Xu, L., Xia, Q., Cao, J., He, J., Zhou, C., Guo, Y., & Pan, D. (2021). Ultrasonic effects on the headspace volatilome and protein isolate microstructure of duck liver, as well as their potential correlation mechanism. *Ultrasonics Sonochemistry, 71*, Article 105358. https://doi.org/10.1016/j.ultsonch.2020.105358

Xue, C., You, J., Zhang, H., Xiong, S., Yin, T., & Huang, Q. (2021). Capacity of myofibrillar protein to adsorb characteristic fishy-odor compounds: Effects of concentration, temperature, ionic strength, pH and yeast glucan addition. *Food Chemistry, 363*, Article 130304. https://doi.org/10.1016/j.foodchem.2021.130304

Yang, Q., Lou, X., Wang, Y., Pan, D., Sun, Y., & Cao, J. (2017). Effect of pH on the interaction of volatile compounds with the myofibrillar proteins of duck meat. *Poultry Science, 96*(6), 1963–1969. https://doi.org/10.3382/ps/pew413

Yousef, R. I., El-Eswed, B., & Ala'a, H. (2011). Adsorption characteristics of natural zeolites as solid adsorbents for phenol removal from aqueous solutions: Kinetics, mechanism, and thermodynamics studies. *Chemical Engineering Journal, 171*(3), 1143–1149. https://doi.org/10.1016/j.cej.2011.05.012

Yu, X., Cai, X., Li, S., Luo, L., Wang, J., Wang, M., & Zeng, L. (2022). Studies on the interactions of theaflavin-3, 3′-digallate with bovine serum albumin: Multi-spectroscopic analysis and molecular docking. *Food Chemistry, 366*, Article 130422. https://doi.org/10.1016/j.foodchem.2021.130422

Zhang, L., Sun, J., Qi, Y., Song, Y., Yang, Z., Li, Z., … Zhou, G. (2020). Forming nanoconjugates or inducing macroaggregates, curcumin dose effect on myosin assembling revealed by molecular dynamics simulation. *Colloids and Surfaces A: Physicochemical and Engineering Aspects, 607*, Article 125415. https://doi.org/10.1016/j.colsurfa.2020.125415

Zhang, H., Wu, D., Huang, Q., Liu, Z., Luo, X., Xiong, S., & Yin, T. (2020). Adsorption kinetics and thermodynamics of yeast β-glucan for off-odor compounds in silver carp mince. *Food Chemistry, 319*, Article 126232. https://doi.org/10.1016/j.foodchem.2020.126232

Zhang, H., Xiong, Y., Bakry, A. M., Xiong, S., Yin, T., Zhang, B., … Huang, Q. (2019). Effect of yeast β-glucan on gel properties, spatial structure and sensory characteristics of silver carp surimi. *Food Hydrocolloids, 88*, 256–264. https://doi.org/10.1016/j.foodhyd.2018.10.010

Zhang, B., Yang, H., Tang, H., Hao, G., Zhang, Y., & Deng, S. (2017). Insights into cryoprotective roles of carrageenan oligosaccharides in peeled whiteleg shrimp (*Litopenaeus vannamei*) during frozen storage. *Journal of Agricultural and Food Chemistry, 65*(8), 1792–1801.